Transportation Geotechnics 31 (2021) 100639

Contents lists available at ScienceDirect

Transportation Geotechnics

journal homepage: www.elsevier.com/locate/trgeo

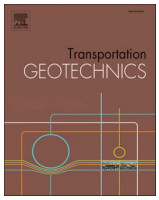

Shear strength and life cycle assessment of volcanic ash-based geopolymer and cement stabilized soil: A comparative study

Pooria Ghadir [a], Mostafa Zamanian [b], Nazanin Mahbubi-Motlagh [b], Mohammad Saberian [c], Jie Li [c], Navid Ranjbar [d,e,*]

[a] Department of Civil Engineering, Iran University of Science and Technology, Tehran, Iran
[b] Faculty of Civil, Water, and Environmental Engineering, Shahid Beheshti University, Iran
[c] Department of Civil and Infrastructure Engineering, RMIT University, Melbourne, Australia
[d] Department of Mechanical Engineering, Technical University of Denmark, 2800 Kgs Lyngby, Denmark
[e] Department of Health Technology, Technical University of Denmark, 2800 Kgs Lyngby, Denmark

ARTICLE INFO

Keywords:
Shear strength
Geopolymer
Soil stabilization
Cement
Clay soil
Life cycle assessment

ABSTRACT

There is a growing interest in developing environmentally-friendly substitution for Portland cement in soil stabilization. This study evaluated the feasibility of using volcanic ash (VA)-based geopolymer as an alternative soil stabilizer to cement by comparing their shear strength behavior and life cycle assessment (LCA). The effects of curing conditions, vertical confinements, binder contents, and alkali activator properties were investigated. The results revealed that regardless of the type of binder, increasing binder content changes the structure of clayey soil through aggregation, thus improves the shear resistance. The interparticle bonds developed faster at higher curing temperatures, and the interlocking of the particles increased at higher confining pressures. Based on the determined boundary conditions, the LCA suggested a comparative environmental impact for both binders to stabilize 1 m^3 functional unit of clayey soil with similar shear strength.

Introduction

Strengthening of soil against shear loading is crucial for the stability of geotechnical profiles. During a shear process, there is a high risk in the breakage of interfacial soil structure when the maximum shear resistance in any plane is only limited to the soil shear strength [1]. To date, several examples of weak shear strength of geological profile registered as sudden landslides which were triggered through rainfall or rise of groundwater level (e.g., 2018 Cebu landslide), earthquakes (e.g., 1999 Tsao-Ling landslide), and by human activities such as building steep embankments and deep tunnels for roads construction (e.g., 2010 landslide on Freeway No. 3, Taiwan) [2,3]. Shear base failure is more likely to occur in soft soils than granular structures due to the reduced cohesion and friction between soft soil particles at a high moisture level [4]. Different mechanical and chemical soil stabilization techniques are employed to prevent such failures. The principle of the mechanical approaches is to increase the friction between the soil particles (e.g., by water drainage) or transferring the internal stress of the soil into stronger elements (e.g., reinforcements) [5,6] while the chemical stabilization approach is to provide strong chemical bonding and surface tension between soil particles using binders [7,8].

Of all binders, cement is the most favored material in soil stabilization techniques. The main reason is its availability and cost-efficiency with respect to mechanical strength. However, complete hydration of cement requires sufficient moisture, which is not always available in geotechnical applications; therefore, the maximum mechanical strength is often not achievable, e.g., in a hot environment [9,10]. Besides, cement production releases a considerable fraction of the total anthropogenic greenhouse gases [11–13]. It has been shown that depending on the clinker to cement ratio, the production of each ton of cement generates ~ 0.5–0.95 t CO_2 [14]. The CO_2 emission related to cement used in geotechnical applications such as soil stabilization and grouting has been counted as about 2 % of the total CO_2 emission by cement. In this line, it has been estimated that replacing 10 % of cement usage with low-carbon materials in geotechnical engineering implementations leads to an annual reduction of 6.1 million tonnes of CO_2 [15]. Therefore, supplementary resources such as fly ash, silica fume, and ground granulated blast furnace slag have been considered partial replacements for cement in geotechnical applications [16–18].

Geopolymer has been emerging as a potential alternative to cement

* Corresponding author at: Department of Mechanical Engineering, Technical University of Denmark, 2800 Kgs Lyngby, Denmark.
E-mail address: naran@mek.dtu.dk (N. Ranjbar).

https://doi.org/10.1016/j.trgeo.2021.100639
Received 3 April 2021; Received in revised form 18 July 2021; Accepted 8 August 2021
Available online 13 August 2021

with less CO_2 footprint for soil stabilization application, produced through alkali activation of aluminosilicate-rich materials [19]. The aluminosilicate precursors obtain from waste materials (e.g., fly ash) or natural resources (e.g., volcanic ash (VA)) that often do not need significant pre-treatment [20,21]. In addition, to tackle the environmental concerns, geopolymer-treated soil has shown enhanced compressive strength in hot environments compared with cement compartments [22]. Recent studies have demonstrated improved shear strength for both cohesive and granular soils when stabilized by geopolymer [23]. Accordingly, the shear strength of high plasticity clay and silty sand has been increased from 800 to 1500 kPa and 1000 to 1800 kPa, respectively, when 10 wt% of the soil was replaced with FA-based geopolymer [23].

Several factors affect the mechanical properties of geopolymers which have been well discussed for the development of concrete. However, in geotechnical applications, the binder to filler ratio is low, and other mechanisms such as aggregation of small particles and interparticle friction play roles in the overall performance of the cemented soil [24]. To this end, this study systematically investigates the significant parameters which influence soil stabilization using VA-based geopolymer, including curing condition and time, vertical confinement, binder content, and mixing parameters of geopolymer, including alkali activator content and sodium hydroxide molarity. The measurements are compared with CEM1. Also, a comparative life cycle assessment (LCA) study on the environmental impacts of the production of two types of binders (i.e., CEM1 and VA-based geopolymer) is conducted.

Material characterization and test procedures

Soil characterization

The particle size analysis of the as-received soil, as performed according to ASTM D 422 [25], shows it contains 5 wt% of gravel, 19 wt% of sand, 33 wt% of silt, and 43 wt% of clay, see Fig. 1a. The soil was used after sieving below 4.75 mm to remove large aggregates. According to the Unified Soil Classification System, the soil was classified as low plasticity clay, CL, see Fig. 1b. The liquid limit (LL), plastic limit (PL), and plasticity index (PI) of the soil was measured as 31%, 22%, and 9%, respectively, according to ASTM D 4318 [26]. The optimum water content and maximum dry density of the soil were obtained 14 wt% and 1.74 g/cm^3, respectively, in accordance with ASTM D 698 [27] Fig. 1c.

Chemical composition of VA and CEM1

The Taftan Mountain's VA was supplied by Zabol Cement Industries Company and was sieved to below 200 μm. The CEM1 was obtained from Fars Cement Company. The oxide composition of VA and CEM1 are provided in Table 1.

Specimen preparation

To prepare the binders, predetermined concentrations of VA and CEM1 were mixed with sodium hydroxide solution and water, respectively, for 5 min. Then the slurry was mixed with the soil for 10 min to obtain a visually homogeneous mixture. The effect of binder content was investigated by substitution of soil with either VA or CEM1 in 0, 5, 10, and 15 wt%. A constant activator content of 14 wt% of the soil was used for all the specimens. This value was determined the same as the optimum water content of the untreated specimen, see Fig. 1c. Direct shear tests were scheduled in three sets. The role of binder type, binder content, curing time, and curing conditions were investigated in set 1. Sets 2 and 3 explored the effects of alkali activator content and sodium hydroxide concentration on geopolymer treated specimens for long-term curing up to 90 days. Regarding Set 2, VA content and sodium hydroxide solution molarity were fixed at 15 wt% and 8 M, respectively, while the alkali activator to optimum water ratio was varied in the range of 1 to 1.4. At Set 3, two different sodium hydroxide solutions of 8 M and 12 M were selected, while the binder content and alkali activator to optimum water content ratio were kept constant at 15 wt% and 1.4, respectively. The specimens were cured at three different conditions, including dry condition (DC), optimum water condition (OC), and soaked condition (SC) (refer to Table 2). Details of the experiments are shown in Table 3.

Procedure to measure the reactivity of VA

The reactivity of the VA was quantified by measuring the dissolved fraction of VA in sodium hydroxide solution. Therefore, 1 g of VA was first stirred in 100 mL of 8 M sodium hydroxide solution at different temperatures and time ranges of 25 to 105 °C for 1 to 256 h, respectively. Then, the insoluble particles were separated using a centrifuge, washed three times with tap water, dried for 1 h at 250 °C, and weighted [28].

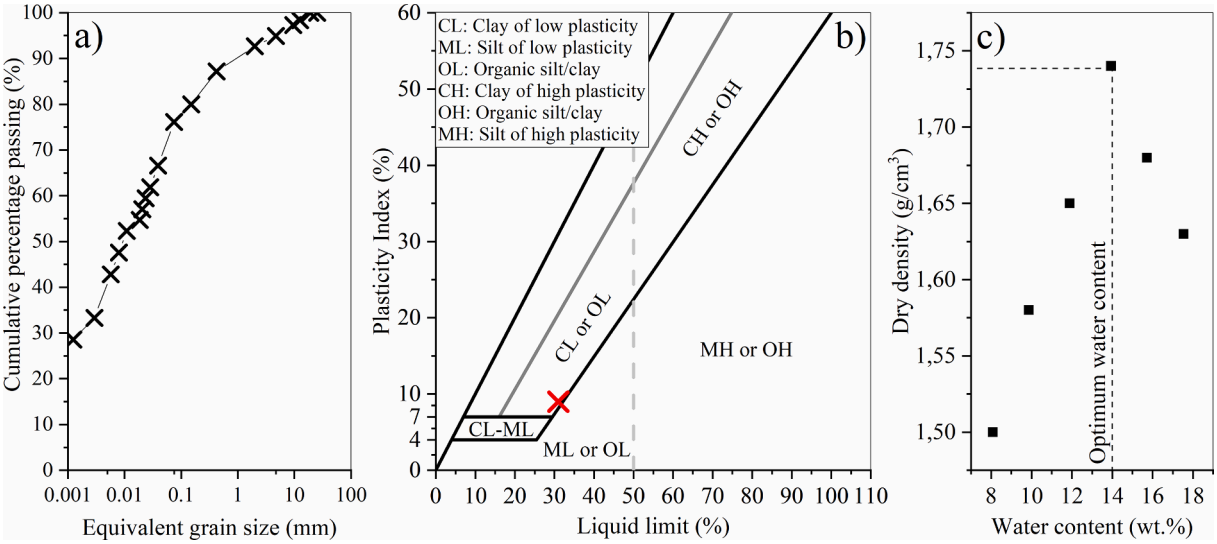

Fig. 1. Soil characterization (a) grain size distribution curve, (b) unified soil classification system, and (c) compaction curve to find the optimum water content.

Table 1
Oxide compositions of VA and CEM1.

Oxide composition	SiO_2	CaO	Al_2O_3	Fe_2O_3	K_2O	Na_2O	MgO	TiO_2	SrO	SO_3	P_2O_5	MnO
VA [wt.%]	46.8	19.1	13.5	8.5	4.3	4.1	1.7	0.9	0.3	0.3	0.2	0.2
CEM1 [wt.%]	11.8	69.6	3.2	8.4	1.4	0.4	2.4	0.3	0.1	1.9	0.0	0.2

Table 2
Curing and test condition of the soil specimens.

Curing type	Curing type	Temperature (°C)	Relative humidity (%)
DC	Oven curing	45 ± 2	15 ± 2
OC	Wrapped by cling film	25 ± 2	80 ± 2
SC	Wrapped by cling film and soaked in water for 24 h before testing	25 ± 2	–

Table 3
Direct shear test schedule in this study.

Material set	Binder type	Binder content [%]	Type of activator	Sodium hydroxide molarity [M]	Testing age [day]	Curing condition	Activator content to optimum water content ratio
Set 1	VA	0, 5, 10, 15	Sodium hydroxide	8	1, 28	DC, OC, SC	1[a]
	CEM1	0, 5, 10, 15	Water	–	1, 28	DC, OC, SC	1
Set 2	VA	15	Sodium hydroxide	8	28, 90	DC, OC, SC	1, 1.2, 1.4
Set 3	VA	15	Sodium hydroxide	8,12	28, 90	DC, OC, SC	1.4

[a] Optimum water content = 14 wt%.

Direct shear test

The direct shear tests were performed using an ELE machine on specimens with 60 × 60 × 20 mm dimensions with three different vertical confinements of 50, 100, and 150 kPa, according to ASTM D 3080 [29]. Shear rates of 0.08 mm/min for SC, and 0.133 mm/min for OC and DC were used. These rates were adopted based on previous research and the consolidation rate of as-received soil [30,31]. A higher loading rate was used for the OC and DC as there was no drainage effect at these conditions. The shear box was kept dry at the OC and DC conditions while it was filled with distilled water at the SC specimens. For the SC condition, the specimens were kept underwater for 24 h before the shear test.

The peak shear strength (τ_f), interparticle cohesion (c), and friction angle (φ) values were determined by direct shear tests using the Mohr-Coulomb criterion as in Eq. (1). In this equation, σ is normal stress acting on the failure surface in the form of vertical confinement.

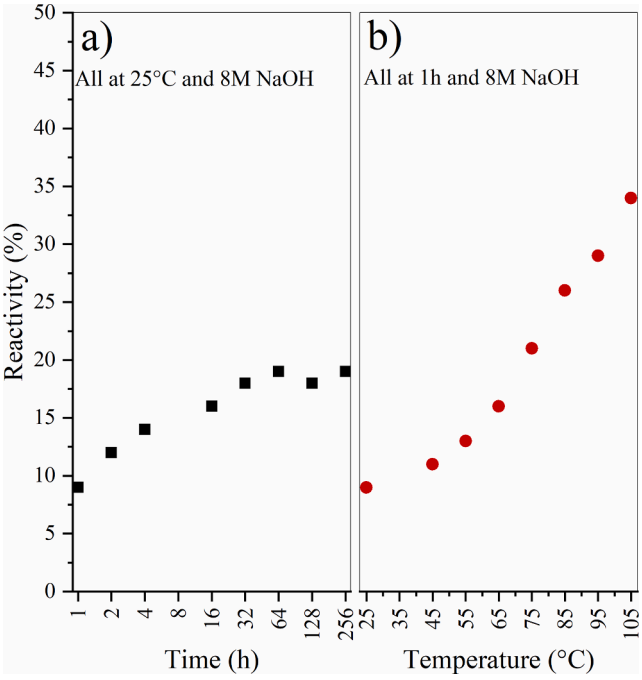

Fig. 2. Reactive phase quantification of VA a) for 1 to 256 h at a constant temperature of 25 °C, b) at different temperatures of 25 to 105 °C for 1 h.

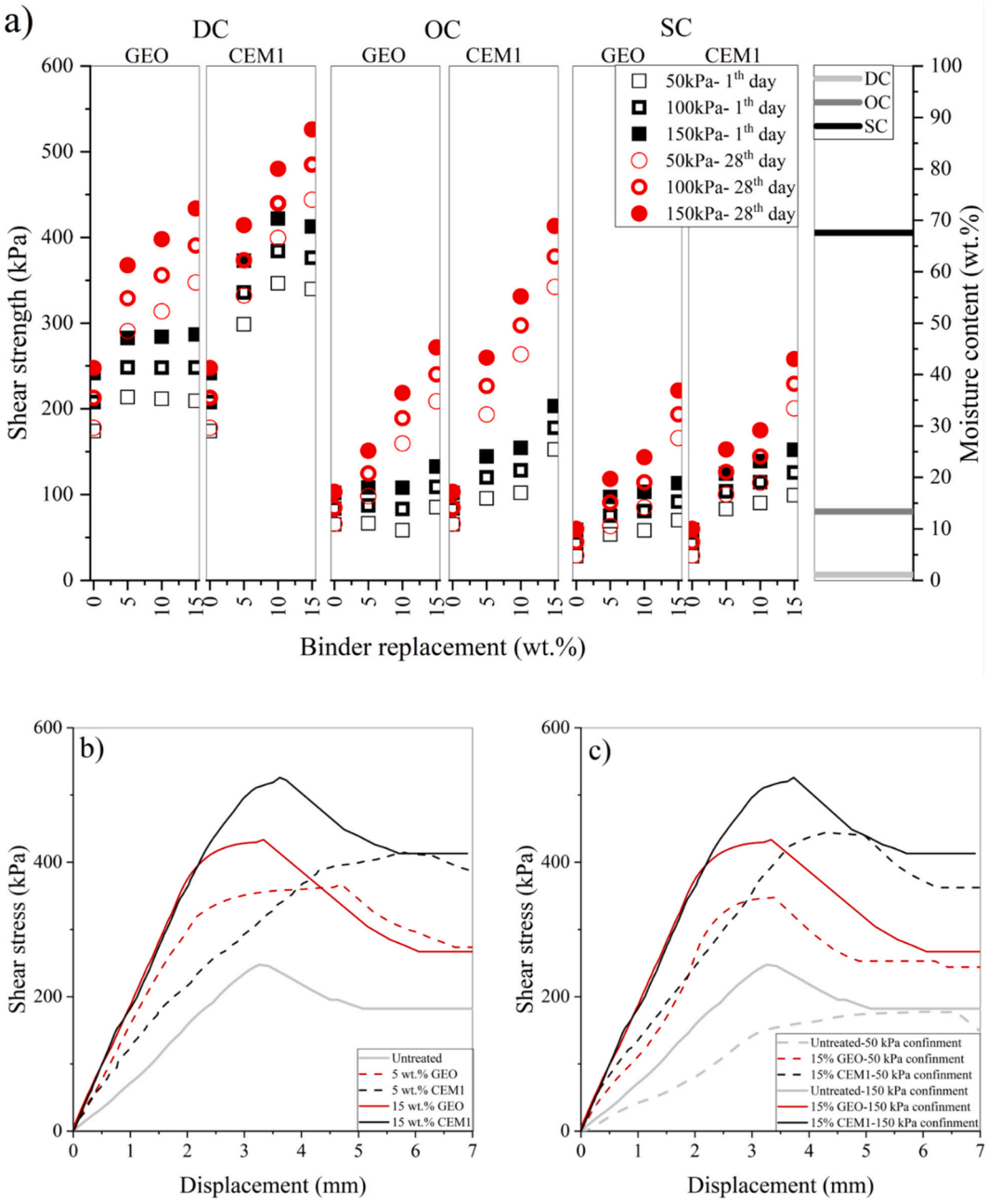

Fig. 3. (a) Peak shear strength and moisture content of untreated and treated soil specimens using geopolymer and CEM1 with different binder content (0 to 15 wt %), curing condition (DC, OC, and SC conditions), and curing duration of 1 and 28 days; (b) and (c) stress-displacement curve of untreated and treated soil specimens using geopolymer and CEM1 with different binder contents and confinements, respectively. All cured at DC for 28 days.

$$\tau_f = c + \sigma tan(\varphi) \quad (1)$$

All specimens were statically compacted into three layers. The moisture content was measured by heating the specimens up to 110 °C for 24 h immediately after the direct shear tests.

A Dino-Lite digital microscope (with 200X magnification) was used to take optical images.

Results

VA reactivity

Fig. 2 shows the low dissolution reactivity of VA at ambient temperature, 25 °C. As observed, only ~ 18 wt% of the material was dissolved after stirring at 8 M NaOH for 32 h, and no more dissolution was observed afterward, Fig. 2a. However, increasing temperatures escalated both amount and rate of dissolution, i.e., the dissolved fraction in 1 h at 65 °C is almost similar to that of dissolved for 256 h at 25 °C, Fig. 2b. The dissolved fraction increased further to ~ 35 wt% at 105 °C for 1 h. This is due to the higher kinetic energy of the system, which eases the breaking of solute molecules by the solvent [28,32].

Shear strength

Fig. 3 presents the peak shear strength and the moisture content of untreated and treated clay specimens cured at different curing conditions of DC, OC, and SC tested at 1 and 28 days. The increase in moisture content from 1 to 14 wt% and above reduced the shear strength of the clayey specimens significantly. This effect was observed in both treated

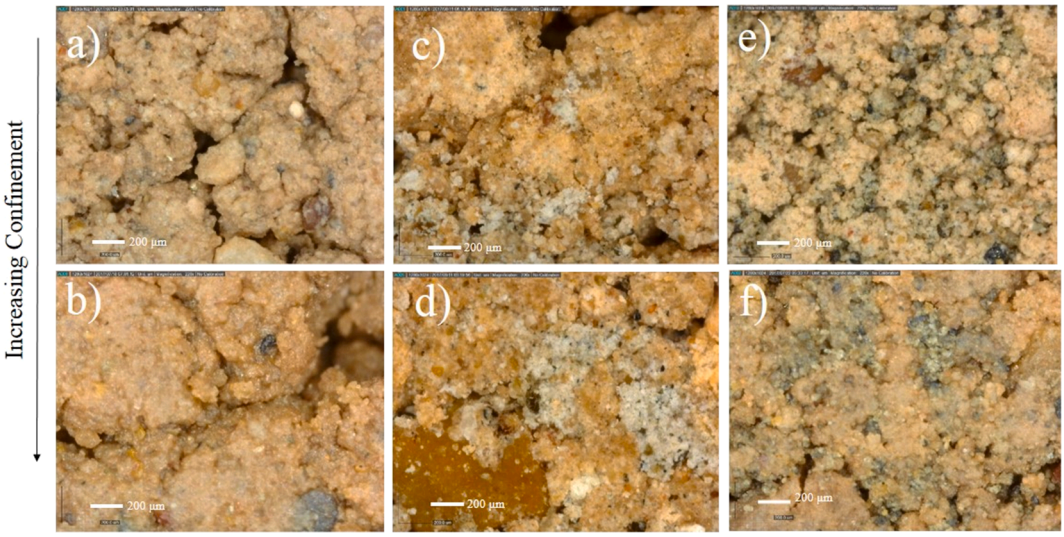

Fig. 4. Optical images of aggregation of (a), (b) untreated, (c), (d) 15 wt% geopolymer, (e), (f) 15 wt% CEM1 treated clay specimens on 28th day of curing at DC curing condition.

and untreated soil specimens.

To investigate the contribution of binder on shear strength of treated soil, the moisture content of the specimens was kept almost constant for each curing condition. As expected, the shear strength was increased in specimens with higher binder content as the binder increases the cohesion forces between soil particles. However, due to the low binder to soil ratio, aggregation of the small particle into larger-size clusters occurred, see Fig. 4 [33]. To this end, the external loads principally were sustained by the large particles, which were closely linked with the movement of fine particles to form the load-carrying capacity of the bulk material [34]. This mechanism was exhibited by an increase in brittleness of the treated soils at higher binder content, see Fig. 3b.

The shear strength increased over time for both binders, however, with different rates depending on curing conditions. At DC, both geopolymer and CEM1 showed comparable shear strength. This was unexpected, as similar geopolymer specimens showed higher compressive strength than CEM1 at higher temperatures [9]. This difference is due to the dominant effect of confinement on the shear performance of soil compared with the uniaxial compressive strength. Hence, higher shear strength and stiffness were registered for all specimens with higher vertical confinements. This is due to a higher required force to reorient the dense soil structure that intensified with the binder effects, see Fig. 3c. At OC, CEM1 specimens showed considerably improved strength after 28 days compared with their geopolymer compartments. Here, sufficient moisture helps to complete the hydration over time. While, as observed in Fig. 2, the reactivity of VA is low at 25 °C and does not increase considerably over time. At SC, the shear strength of treated soil is highly reduced for both binder types as the repelling force due to swelling of soil particles overcome the binding effects.

Cohesion and friction angle

The soil shear behavior can be evaluated in more detail through two components; cohesion or physicochemical bonds and interparticle friction. The overall cohesion is due to the combination of matric suction and effective cohesion. The former is promoting through the combination of negative pore water pressure and surface tension within the water film, while the latter results from interparticle bonds (physicochemical attractions), including cementation and adhesion due to the compaction and electrostatic attractions [35,36]. The internal friction mainly depends on the normal stress acting on the failure surface and the geometrical properties of the particles. The variation of cohesion and friction angle of the specimens subjected to different curing conditions at different ages are shown in Fig. 5.

At DC, the paucity of water causes high capillary and suction forces as the dominant factors in controlling the cohesion within the untreated matrix [37]. Here, the internal friction is mainly induced by the breakdown of aggregates and particle rearrangement under normal stress. Increasing the moisture content from DC to OC increases the separation distance between the clay particles and, thus, decreases the electrostatic attractions (e.g., van der Walls forces) [35]. This was observed as a reduction in both cohesion and friction angle of untreated specimens. At higher moisture content, SC, the capillary suction was completely lost, and the cohesion decreased significantly [35,37]. Furthermore, forming a contractile layer between soil particles reduced the frictional forces [38,39].

In the presence of binders, the effective cohesion of treated soil is escalated by the adhesion of the binders and soil particles [1]. This extra cohesion is less affected by moisture content but binder chemical reactions at different curing conditions. Therefore, for both binders, the cohesion of the treated soils improved by increasing the binder to soil ratio over time. However, as a comparison, a higher cohesion was observed in CEM1 incorporated specimens, especially where the water content was lower. Interestingly, both binders showed almost similar behavior on friction angle. For instance, at DC, the friction angle of the treated specimens was remained constant at 34-41°, independent of the binder content and type. This may be due to the high binder content used in this study compared with the minimum amount of binder needed to form aggregation, change the bulk material structure, and increase the friction angle. A similar increase in friction angle was observed by other researchers through increasing the particle size of the bulk soil [40]. Noteworthy, the small size shear box used in this study resulted in higher values of friction angle and cohesion [41].

Fig. 6a shows that an increase in activator content accelerates the strength development at all curing conditions as a higher number of particles were exposed to the activation environment [42]. Noteworthy, increasing the activator content above a specific value had an adverse effect on the mechanical strength of the bulk soil due to poor compaction [43,44]. Furthermore, Fig. 6b shows that a higher concentration of activation solution improves the long-term shear strength of the specimens, which is associated with the higher dissolution of VA. Similar results were reported by others [43,45].

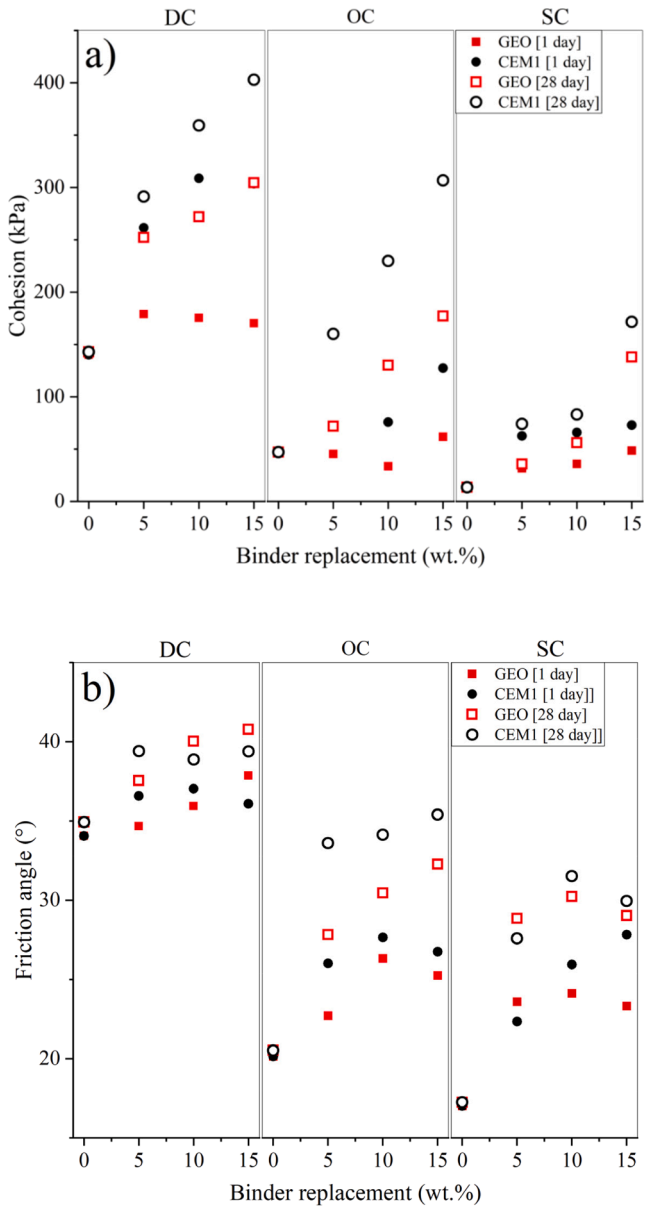

Fig. 5. (a) Cohesion and (b) friction angle of untreated and treated soil specimens using geopolymer and CEM1 with different binder content (0 to 15 wt%), curing condition (DC, OC, and SC conditions), and curing duration of 1 and 28 days.

General discussion on shear behavior of CEM1 and geopolymer stabilized clayey soil

An increase in moisture content reduces capillary force and effective normal stress on the potential failure surface of the soil bulk, and therefore, degrades the shear strength. This phenomenon is more significant in clayey soils due to their interlayer ionic charges, which provide the basis of water adsorption in the form of hydrosphere surround the particles to swell [46]. The thickness of the adsorbed water layer is ~ 1 to 2.2 nm and formed at a water content range of ~ 15 to 25 wt%. These values depend on several factors, including layer charge, interlayer cations, properties of adsorbed liquid and particle size, and environmental temperature [47,48]. In the presence of water, the repulsion between the swelled clay particles removes the frictional contacts observed in dry states. This can be observed in Fig. 5b, where the friction angle of the untreated clay significantly reduced at a high moisture content of OC. Increasing the water content beyond the plastic limit does not influence much on the shear strength and friction angle of the soil, Fig. 3a and 5b [49,50].

According to Mohr's criterion, a material yields when its stress circle tangent to the failure envelope. Shear is the main state of stress-causing failure in cohesive-frictional solids, such as clayey soils. This usually takes place on the planes of maximum shear or as a combination with compressive or tensile stresses, Fig. 7a. To this end, higher shear strength is observed at higher confinement, see Fig. 3c. When the confinement is low, the soil structure is porous, and particles are free to move, while increasing the confinement results in a compact structure with high frictional interaction that limits particles' dislocation. Therefore, the shear surface forms only if the mineral friction and mechanical interlock between adjacent soil particles are overcome, or the particles are broken [51]. When a binder is used, the shear strength is increased since higher energy is required to break the interparticle bonds and the shear surface is extended. This was shown by the increase in the cohesion of treated specimens, see Fig. 5a. In addition to the interparticle bonds, the binder changes the structure of the clayey mass through the aggregation of clay particles that increase the friction in the bulk mass. Interestingly, this was less dependent on the range of binder content used in this study. A summary of the effect of confinement on shear strength is seen in Fig. 7b.

The performance of stabilized soil subjected to shear is not necessarily similar to that of compression at different curing conditions. The uniaxial compressive strength of treated soil predominantly depends on the binder strength. Therefore, high compressive strength is observed for geopolymer specimens cured at hot and dry condition while in a wet environment for CEM1 [9]. However, the strength of the soil is highly influenced by vertical confinement, and therefore, the trend observed for uniaxial compression was not the same for shear. A similar trend of shear strength, friction angle, and cohesion was observed for both geopolymer and CEM1 at DC. Besides, since the binder content is not enough to cover all the clay particles, repulsion force, due to the formation of the adsorbed layer, controlled the behavior of the treated soils at high moisture contents. However, CEM1 specimens showed an improved behavior at OC, which provides enough bonds to overcome the swelling force of clays at such moisture contents, Fig. 7c. This strength is expected to develop over time for the VA-based geopolymer due to the slow rate of reaction at low temperatures.

Life Cycle Assessment (LCA)

Goal and scope definition

A comparative estimation of environmental impacts of the binders, CEM1 and VA-based geopolymer, has been performed using LCA. It is worth mentioning that the life cycle assessment (LCA) framework was chosen to assess the environmental impacts of the products according to the standard [52]. The scope of LCA in this study is limited to the production of the required CEM1 and VA-based geopolymer for stabilization of 1 m^3 functional unit of clayey soil with similar shear strength. Since this LCA study deals with production systems, the cradle-to-gate theory was followed. System boundary included energy required for CEM1 production (i.e., quarrying limestone, transportation to cement production plant, crushing, and cement production process), VA extraction/quarrying, transportation to the plant, and grinding, as well as NaOH production and its transportation, as illustrated by solid lines in Fig. 8. While the required energy for transporting the materials to a construction site, site preparation, mixing the binders with soil, soil compaction, and service phase was not considered, as shown by dotted lines in Fig. 8. The transportation of quarried materials to the plants was assumed 100 km for all the raw materials. Fig. 8 shows the system boundary considered for this LCA methodology.

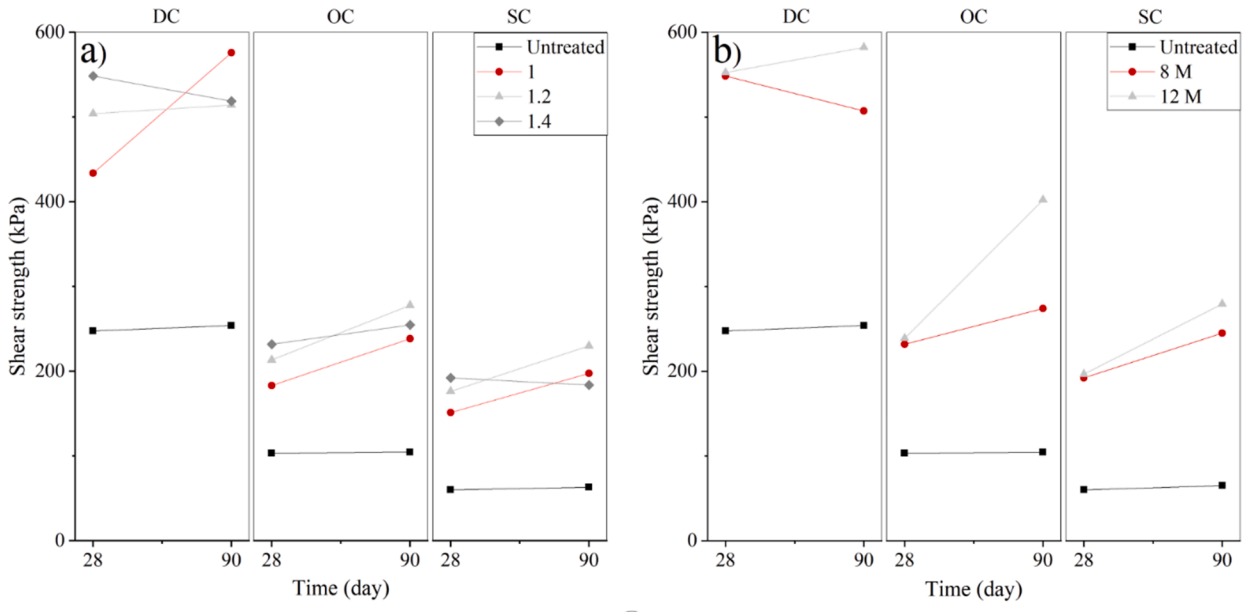

Fig. 6. (a) Effect of activator content, and (b) concentration of sodium hydroxide on shear strength of untreated and treated soil specimens using geopolymer at DC, OC, and SC curing conditions, and curing duration of 28 and 90 days. The vertical confinement was 150 kPa for all the samples.

Life Cycle Inventory (LCI) data

At this stage of the LCA, it is necessary to collect all inputs and outputs of the productive system [53]. All the Life Cycle Inventory (LCI) data for VA were collected from the local mining and the VA production company. In the Taftan mine, diesel is used for mining machinery, and a grinding process is used on the raw VA rocks. For electricity production in Iran, data were obtained from [54]. Also, secondary data, like the Ecoinvent v.3 database, were used for missing and non-accessible data. The SimaPro input data were used for CEM1 and NaOH. Moreover, it is worth mentioning that the soil's maximum dry density was 1740 kg/m^3 in accordance with ASTM D 698 [27], Fig. 1c. Considering that most of the studied area (Iran country) located in arid zones and based on the experimental results of this study, it was observed that at DC curing condition, two blends of the soil stabilized with 5% CEM1 and treated with 10% VA-based geopolymer provided the almost similar 28-day shear strength values at all vertical confinements. Therefore, the CEM1 and water needed to stabilize 1 m^3 clayey soil were 87 kg and 243.6 kg, respectively. Comparatively, 174 kg VA, 59.2 kg NaOH, and 184.4 kg water were required for VA-based geopolymer.

Life cycle impact assessment and interpretation of the results

The life cycle impact assessment is useful for estimating the resources used and evaluating the potential environmental impacts in the modeled system. The life cycle impact assessment was conducted using the SimaPro software. The reported life cycle impact assessment of the two products shows their environmental impacts in terms of 11 impact categories, which are obtained using the problem-oriented (mid-points) methodology (ReCiPe midpoint (H) method version 1.12).

Table 4 provides the ReCiPe midpoint (H) method results for CEM1 and VA-based geopolymer production in different categories. Subsequently, Fig. 9 shows the percentage contributions by different life cycle inventory of both products. The contribution to climate change is almost similar for CEM1 and VA in this study. The CEM1 production is making up 51% of the total emitted CO_2, which is mainly due to the decomposition of $CaCO_3$ during the production of cement clinker, which releases up to 60% of the total CO_2 [55]. Furthermore, this is an energy-intensive process [56]. On the other side, the main contributor to the environmental impacts of VA-based geopolymer, $CO_{2\text{-eq}}$, $SO_{2\text{-eq}}$, $PM_{10\text{-eq}}$, and $CFC\text{-}_{11\text{-eq}}$ emissions is the activation solution. This result is in agreement with previous studies [57,58]. There are, however, two points that need to be considered: I) the amount of geopolymer binder used in this study was twice compared with the CEM1 with almost the same shear strength in the timeframe of 28 days. However, it is known that VA has a slow reaction rate in low temperatures, see Fig. 2b, and different results will be obtained in the long term. II) The calculation in this study is unique to the stabilization for similar shear strength, and different values are expected for other comparative indices, e.g., in the previous study, a similar VA-based geopolymer outperformed CEM1 in uniaxial compressive strength (28-day compressive strength of the soil stabilized with 5% VA-based geopolymer was more than 2.5 times than that of the soil treated with 5% CEM1 at DC curing condition) [9]. This means a comparative LCA is a nontrivial task as it not only depends on compositions but also the application and condition. However, it is obvious that using activation solutions processed with less environmental impacts, such as NaOH made from solar salt [57] and waste-derived waterglass [60,61], or using more reactive aluminosilicate sources, such as fly ash and slag, are the way of future for the development of environmentally friendly geopolymer binders for soil stabilization [57,59].

Conclusions

This study investigated the potential of using VA-based geopolymer as an alternative green binder to the conventional cement for soil stabilization by assessing shear strength parameters. The effects of binder content (0 to 15 wt%), curing conditions (at dry, optimum water content, and soaked conditions), vertical confinement (50 to 150 kPa), and curing duration were examined for two types of binders, VA-based geopolymer and CEM1. The results showed that independent of the binder type, the shear strength of treated specimens was improved at higher binder content, longer curing duration, and lower moisture content. The increase in shear strength was explained based on the changes in cohesion and friction of the bulk soil. It was demonstrated that the overall cohesion force of the treated soil particles was mainly affected by the binder parameters, including curing condition, binder content, alkali activator content, and concentration. Furthermore, incorporation of the binder caused aggregation of the clay particles into larger-size clusters, which changed the bulk material's structure. This

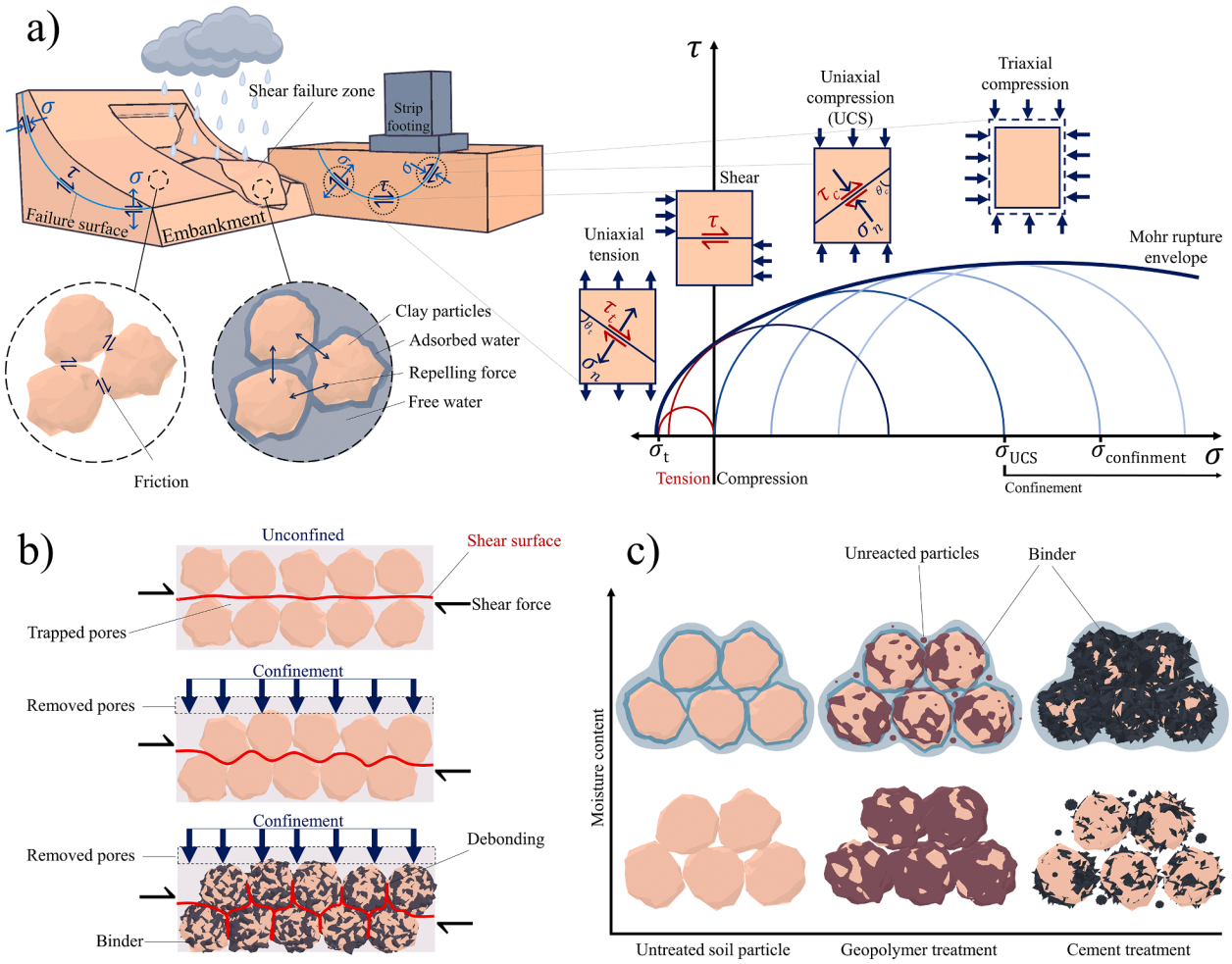

Fig. 7. Schematic diagram of (a) stress distribution at failure surfaces of geotechnical profiles, (b) confinement effect on shear surface development in untreated and treated soil, (c) performance of binders at different curing conditions.

aggregation increased the interparticle friction and was less dependent on the binder type and content at the limits of this study. However, in the presence of water, the repulsion forces between clay particles overcame the chemical bonds and reduced both cohesion and friction of the soil. The LCA results estimated similar climate change impacts for CEM1 and VA-based geopolymer used in this study for stabilization of 1 m^3 functional unit of clayey soil with similar shear strength. This LCA, however, was unique to the boundary conditions of this study. Regardless of the boundary conditions, the main contributor to the environmental impacts in the geopolymer matrix was the activation solution which needs to be investigated further in the development of environmentally friendly geopolymer binders for soil stabilization.

CRediT authorship contribution statement

Pooria Ghadir: Conceptualization, Validation, Investigation, Writing – original draft, Writing – review & editing. **Mostafa Zamanian:** Methodology, Validation, Resources, Writing – review & editing. **Nazanin Mahbubi-Motlagh:** Methodology, Investigation. **Mohammad Saberian:** Methodology, Investigation, Writing – original draft. **Jie Li:** Resources, Writing – review & editing. **Navid Ranjbar:** Conceptualization, Writing – original draft, Writing – review & editing, Supervision.

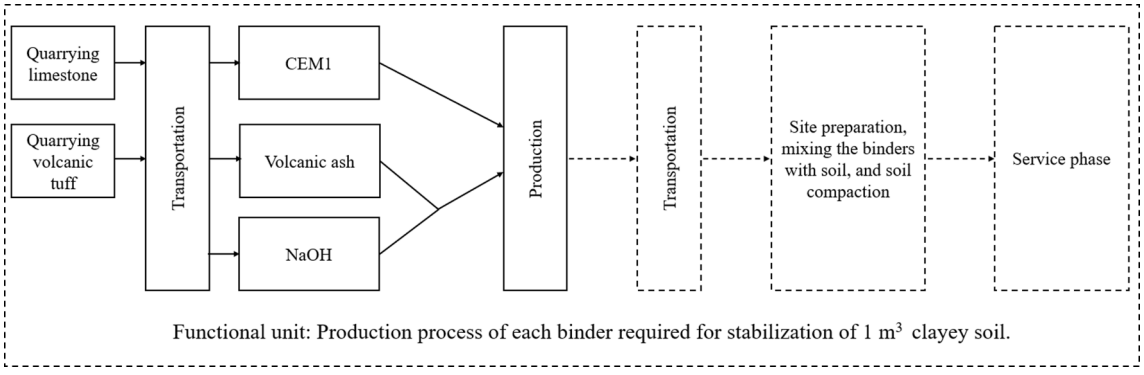

Fig. 8. The system boundary considered for this LCA.

Table 4
ReCiPe midpoint (H) method results for CEM1 and VA-based geopolymer for stabilization of 1 m^3 functional unit of clayey soil with similar shear strength.

Impact categories	CEM1			VA-based geopolymer				
	Total	Transport of limestone (100 km)	Cement production (87 kg)	Total	Transport of volcanic materials (100 km)	VA production (174 kg)	Transport of NaOH raw materials (100 km)	NaOH production (59.2 kg)
Climate change (kg CO_2 eq)	78.222	0.806	77.415	75.105	1.613	7.978	0.549	64.965
Ozone layer depletion (kg CFC-11 eq)	2.586×10^{-6}	3.047×10^{-11}	2.585×10^{-6}	8.392×10^{-6}	6.095×10^{-11}	1.248×10^{-7}	2.074×10^{-11}	8.267×10^{-6}
Terrestrial acidification (kg SO_2 eq)	0.14341	0.00407	0.13934	0.59618	0.00814	0.04959	0.00277	0.53566
Marine eutrophication (kg N eq)	0.00687	0.00021	0.00665	0.00716	0.00043	0.00077	0.00015	0.00580
Human toxicity (kg 1,4-DB eq)	7.591	0.412	7.179	15.258	0.825	2.395	0.28077	11.756
Photochemical oxidant formation (kg NMVOC)	0.14654	0.00603	0.14050	0.22678	0.01206	0.02404	0.00411	0.18656
Particulate matter formation (kg PM10 eq)	0.06026	0.00147	0.05878	0.14785	0.00295	0.01298	0.00101	0.13090
Terrestrial ecotoxicity (kg 1,4-DB eq)	0.00221	9.462×10^{-7}	0.00220	0.00095	1.893×10^{-6}	0.00009	6.439×10^{-7}	0.00085
Freshwater ecotoxicity (kg 1,4-DB eq)	0.17783	0.00342	0.17441	0.13448	0.00684	0.02452	0.00233	0.10077
Marine ecotoxicity (kg 1,4-DB eq)	0.17468	0.00336	0.17131	0.13052	0.00673	0.02419	0.00229	0.09730
Metal depletion (kg Fe eq)	0.66035	0	0.66035	0.02559	0	0.02559	0	0

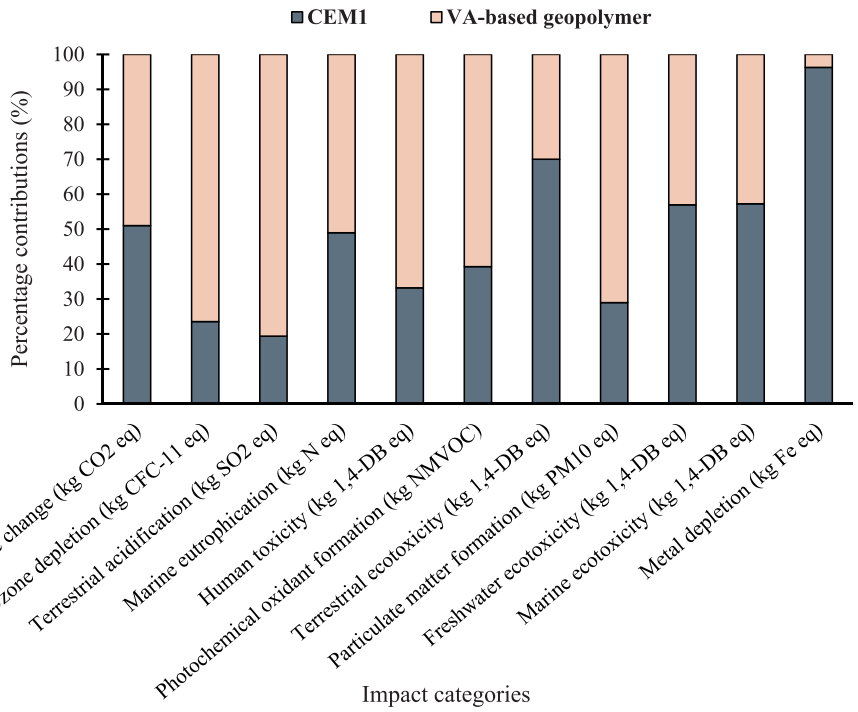

Fig. 9. Percentage contributions of each impact category for CEM1 and VA-based geopolymer based on the data in Table 4.

Declaration of Competing Interest

The authors declare that they have no known competing financial interests or personal relationships that could have appeared to influence the work reported in this paper.

Acknowledgment

N. Ranjbar has received funding from the European Union's Horizon 2020 research and innovation program under the Marie Sklodowska-Curie grant agreement no. 713683 (COFUNDfellowsDTU). Also, the authors would like to acknowledge the National Elites Foundation of Iran.

References

[1] Lian B, Peng J, Zhan H, Wang X. Mechanical response of root-reinforced loess with various water contents. Soil Tillage Res 2019;193:85–94.
[2] Hung J-J. Chi-Chi earthquake induced landslides in Taiwan. Earthquake Eng Eng Seismology 2000;2(2):25–33.
[3] Wang L, Hwang JH, Luo Z, Juang CH, Xiao J. Probabilistic back analysis of slope failure–A case study in Taiwan. Comput Geotech 2013;51:12–23.
[4] Stark TD, Choi H, McCone S. Drained shear strength parameters for analysis of landslides. J Geotech Geoenviron Eng 2005;131(5):575–88.
[5] Farhangi V, Karakouzian M, Geertsema M. Effect of micropiles on clean sand liquefaction risk based on CPT and SPT. Appl Sci 2020;10(9):3111.
[6] Saberian M, et al. Application of demolition wastes mixed with crushed glass and crumb rubber in pavement base/subbase. Resour Conserv Recycl 2020;156:104722.
[7] Hataf N, Ghadir P, Ranjbar N. Investigation of soil stabilization using chitosan biopolymer. J Cleaner Prod 2018;170:1493–500.
[8] MolaAbasi H, et al. Evaluation of the long-term performance of stabilized sandy soil using binary mixtures: A micro-and macro-level approach. J Cleaner Prod 2020:122209.
[9] Ghadir P, Ranjbar N. Clayey soil stabilization using geopolymer and Portland cement. Constr Build Mater 2018;188:361–71.
[10] Pourakbar S, et al. Model study of alkali-activated waste binder for soil stabilization. Int J Geosynthetics Ground Eng 2016;2(4):35.
[11] Roychand R, et al. Development of zero cement composite for the protection of concrete sewage pipes from corrosion and fatbergs. Resour Conserv Recycl 2021;164:105166.
[12] Gartner E. Industrially interesting approaches to "low-CO2" cements. Cem Concr Res 2004;34(9):1489–98.
[13] Shariatmadari N, et al. Experimental study on the effect of chitosan biopolymer on sandy soil stabilization. in E3S Web of Conferences. 2020. EDP Sciences.
[14] Worrell E, et al. Carbon dioxide emissions from the global cement industry. Annu Rev Energy Env 2001;26(1):303–29.
[15] Chang I, Im J, Cho G-C. Introduction of microbial biopolymers in soil treatment for future environmentally-friendly and sustainable geotechnical engineering. Sustainability 2016;8(3):251.
[16] Jahandari S, Saberian M, Zivari F, Li J, Ghasemi M, Vali R. Experimental study of the effects of curing time on geotechnical properties of stabilized clay with lime and geogrid. Int J Geotech Eng 2019;13(2):172–83.
[17] Rezazadeh Eidgahee D, Rafiean AH, Haddad A. A novel formulation for the compressive strength of IBP-based geopolymer stabilized clayey soils using ANN and GMDH-NN approaches. Iranian J Sci Technol, Trans Civil Eng 2020;44(1):219–29.
[18] Abdullah HH, et al. Cyclic behaviour of clay stabilised with fly-ash based geopolymer incorporating ground granulated slag. Transp Geotech 2021;26:100430.
[19] Suksiripattanapong C, et al. Evaluation of polyvinyl alcohol and high calcium fly ash based geopolymer for the improvement of soft Bangkok clay. Transp Geotech 2021;27:100476.
[20] Rivera JF, et al. Fly ash-based geopolymer as A4 type soil stabiliser. Transp Geotech 2020;25:100409.
[21] Wattez T, et al. Interactions between alkali-activated ground granulated blastfurnace slag and organic matter in soil stabilization/solidification. Transp Geotech 2021;26:100412.
[22] Yaghoubi M, Arulrajah A, Disfani MM, Horpibulsuk S, Darmawan S, Wang J. Impact of field conditions on the strength development of a geopolymer stabilized marine clay. Appl Clay Sci 2019;167:33–42.
[23] Thiha S, Lertsuriyakul C, Phueakphum D. Shear strength enhancement of compacted soils using high-calcium fly ash-based geopolymer. Int J Geomate 2018;15(48):1–9.
[24] Amiri E, Emami H. Shear strength of an unsaturated loam soil as affected by vetiver and polyacrylamide. Soil Tillage Res 2019;194:104331.
[25] ASTM D422-63, in Standard Test Method for Particle-Size Analysis of Soils. ASTM 2007: ASTM International, West Conshohocken, PA.
[26] ASTM D4318-17e1, in Standard Test Methods for Liquid Limit, Plastic Limit, and Plasticity Index of Soils. ASTM 2017: ASTM International, West Conshohocken, PA.
[27] ASTM D698-12e2, in Standard Test Methods for Laboratory Compaction Characteristics of Soil Using Standard Effort (12 400 ft-lbf/ft3 (600 kN-m/m3)). ASTM 2012: ASTM International, West Conshohocken, PA.
[28] Kuenzel C, Ranjbar N. Dissolution mechanism of fly ash to quantify the reactive aluminosilicates in geopolymerisation. Resour Conserv Recycl 2019;150:104421.
[29] ASTM D3080M-11, in Standard Test Method for Direct Shear Test of Soils Under Consolidated Drained Conditions. ASTM 2011: ASTM International, West Conshohocken, PA.
[30] Chang Ilhan, Cho Gye-Chun. Shear strength behavior and parameters of microbial gellan gum-treated soils: from sand to clay. Acta Geotech 2019;14(2):361–75.
[31] Ghadakpour M, Choobbasti AJ, Kutanaei SS. Experimental study of impact of cement treatment on the shear behavior of loess and clay. Arabian J Geosci 2020;13(4):184.
[32] Ranjbar Navid, Kashefi Amin, Maheri Mahmoud R. Hot-pressed geopolymer: Dual effects of heat and curing time. Cem Concr Compos 2018;86:1–8.
[33] Elandaloussi R, et al. Effectiveness of lime treatment of coarse soils against internal erosion. Geotech Geol Eng, 2019. 37(1): p. 139-154.
[34] Guo Ning, Zhao Jidong. The signature of shear-induced anisotropy in granular media. Comput Geotech 2013;47:1–15.
[35] Al-Shayea Naser A. The combined effect of clay and moisture content on the behavior of remolded unsaturated soils. Eng Geol 2001;62(4):319–42.
[36] Zhang B, et al. Shear strength of surface soil as affected by soil bulk density and soil water content. Soil Tillage Res 2001;59(3–4):97–106.
[37] Aluko OB, Koolen AJ. The essential mechanics of capillary crumbling of structured agricultural soils. Soil Tillage Res 2000;55(3-4):117–26.
[38] Alonso EE, Pereira J-M, Vaunat J, Olivella S. A microstructurally based effective stress for unsaturated soils. Géotechnique 2010;60(12):913–25.
[39] Fasinmirin Johnson Toyin, Olorunfemi Idowu Ezekiel, Olakuleyin Fasilat. Strength and hydraulics characteristics variations within a tropical Alfisol in Southwestern Nigeria under different land use management. Soil Tillage Res 2018;182:45–56.
[40] Wei Yujie, Wu Xinliang, Cai Chongfa. Splash erosion of clay–sand mixtures and its relationship with soil physical properties: The effects of particle size distribution on soil structure. Catena 2015;135:254–62.
[41] Ziaie Moayed R, Alibolandi M, Alizadeh A. Specimen size effects on direct shear test of silty sands. Int J Geotech Eng 2017;11(2):198–205.
[42] Guo Xiaolu, Shi Huisheng, Dick Warren A. Compressive strength and microstructural characteristics of class C fly ash geopolymer. Cem Concr Compos 2010;32(2):142–7.
[43] Cristelo Nuno, Glendinning Stephanie, Miranda Tiago, Oliveira Daniel, Silva Rui. Soil stabilisation using alkaline activation of fly ash for self compacting rammed earth construction. Constr Build Mater 2012;36:727–35.
[44] Sukmak Patimapon, Horpibulsuk Suksun, Shen Shui-Long. Strength development in clay–fly ash geopolymer. Constr Build Mater 2013;40:566–74.
[45] Hu Mingyu, Zhu Xiaomin, Long Fumei. Alkali-activated fly ash-based geopolymers with zeolite or bentonite as additives. Cem Concr Compos 2009;31(10):762–8.
[46] Martin RT. Adsorbed water on clay: A review, in Clays and Clay Minerals, E. Ingerson, Editor. 1962, Pergamon. p. 28-70.
[47] Villar MV, Lloret A. Influence of temperature on the hydro-mechanical behaviour of a compacted bentonite. Appl Clay Sci 2004;26(1–4):337–50.
[48] Anderson Duwayne M, Low Philip F. The density of water adsorbed by lithium-, sodium-, and potassium-bentonite 1. Soil Sci Soc Am J 1958;22(2):99–103.
[49] Yong R. Soil suction and soil-water potentials in swelling clays in engineered clay barriers. Eng Geol 1999;54(1–2):3–13.
[50] Kong L, Tan L. Study on shear strength and swelling-shrinkage characteristic of compacted expansive soil. Unsaturated Soils For Asia. Singapore 2000:515–9.
[51] Dove J, Bents D, Wang J, Gao B. Particle-scale surface interactions of non-dilative interface systems. Geotext Geomembr 2006;24(3):156–68.
[52] Environmental Management: Life Cycle Assessment; Principles and Framework. ISO 2006, International Organization for Standardization: ISO 14040.
[53] Pradhan Subhasis, Tiwari BR, Kumar Shailendra, Barai Sudhirkumar V. Comparative LCA of recycled and natural aggregate concrete using Particle Packing Method and conventional method of design mix. J Cleaner Prod 2019;228:679–91.
[54] https://www.iea.org/countries/Iran. IEA 2018.
[55] Teh Soo Huey, Wiedmann Thomas, Castel Arnaud, de Burgh James. Hybrid life cycle assessment of greenhouse gas emissions from cement, concrete and geopolymer concrete in Australia. J Cleaner Prod 2017;152:312–20.
[56] Stafford Fernanda N, Raupp-Pereira Fabiano, Labrincha João A, Hotza Dachamir. Life cycle assessment of the production of cement: a Brazilian case study. J Cleaner Prod 2016;137:1293–9.
[57] Salas Daniel A, Ramirez Angel D, Ulloa Nestor, Baykara Haci, Boero Andrea J. Life cycle assessment of geopolymer concrete. Constr Build Mater 2018;190:170–7.
[58] Passuello Ana, Rodríguez Erich D, Hirt Eduardo, Longhi Márlon, Bernal Susan A, Provis John L, et al. Evaluation of the potential improvement in the environmental footprint of geopolymers using waste-derived activators. J Cleaner Prod 2017;166:680–9.
[59] Habert G, d'Espinose de Lacaillerie JB, Roussel N. An environmental evaluation of geopolymer based concrete production: reviewing current research trends. J Cleaner Prod 2011;19(11):1229–38.
[60] Abdulkareem M, et al. Environmental and economic perspective of waste-derived activators on alkali-activated mortars. J Cleaner Prod 2020;280:124651.
[61] Tchakouté Hervé Kouamo, Rüscher Claus Henning, Kong Sakeo, Ranjbar Navid. Synthesis of sodium waterglass from white rice husk ash as an activator to produce metakaolin-based geopolymer cements. J Build Eng 2016;6:252–61.